

ESTIMATION OF TRANSVERSE COUPLING FROM PINHOLE IMAGES

X. R. Resende, P. F. Tavares
 LNLS, Campinas SP 13083-100 Brazil

Abstract

In this paper we report on preliminary results of an ongoing effort at the Brazilian Synchrotron Light Laboratory to better understand and control the residual transverse coupling in the storage ring. In this work we concentrate on the correct interpretation of pinhole images, as a mean of probing beam size and coupling.

INTRODUCTION

The Brazilian Synchrotron Light Laboratory (LNLS) has recently started filling its storage ring straight sections with insertion devices. Last year a 2-Tesla Wiggler was successfully installed and integrated in the control system. An elliptically polarizing undulator is now under construction and scheduled to be installed in the next shutdown, by the end of the current year. The VUV beamline for the undulator is very demanding with respect to orbit stability and other beam parameters. Considerable reduction of the vertical emittance via reduction of the transverse coupling is a must in order for the undulator beamline to achieve its promised outstanding performance. For this purpose a systematic study of the residual coupling has been initiated.

Two experimental methods of probing the coupling were used. The simplest one consists in traditional measurements of tune separation. Although very straightforward in its interpretation, this method can not be used to give beam-line users independent on-line information about beam sizes. In the second method, we used the image of a pinhole formed on the CCD of a X-ray camera in order to extract beam parameters such as beam sizes, emittances, global coupling, coupling angle, etc. This method, contrary to the first one, gives much more information about the beam but it also requires a much more elaborate interpretation in order to yield consistent results. In the third section of this paper we describe our recent efforts in this direction.

MINIMUM TUNE SEPARATION

Traditionally, the estimation of coupling strength in storage rings is done with the measurement of the minimum tune separation. This is accomplished by varying the optics of the ring in a way that the uncoupled tunes cross each other. Due to coupling, the actual tunes never cross and their minimum separation quantifies the coupling strength[1].

We performed such experiment for low beam currents, ≈ 30 mA, in two different configurations: opened and closed wiggler gap. The results are plotted in Fig. 1. In the plot, each point corresponds to one pair of horizontal and ver-

tical tune shifts. The shifts were chosen in such a way that the uncoupled tune separation Δ crossed zero. For each tune shift the quadrupole strengths were slightly re-adjusted. The coupling calculated from the minimum tune separation is 0.29 % for opened wiggler gap and 0.88 % for closed gap. These values do not change significantly when the same experiment is repeated with beam currents that are typically supplied to beam-line users in the beginning of shifts (around 250 mA).

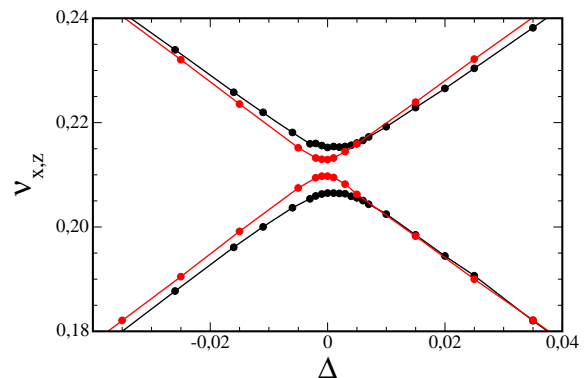


Figure 1: Measurement of minimum tune separation. Red points were obtained for a wiggler configuration with opened gap. Black points correspond to tune measurements for closed gap. The two upper curves are the horizontal tunes, whereas the two lower ones are the vertical tunes.

PINHOLE IMAGE

A grid of pinholes is installed in a beam-diagnostic dedicated beam-line (DFX) $l_1 = 8.5$ meters away from a 15° dipole exit (each LNLS dipole deflects the e-beam by 30°). Each X-ray pinhole image is converted to a digitalized computer image by an in-line $\text{\textcircled{C}}$ SESO XBM camera located at $l_2 = 12.75$ meters from the source.

The pinholes in the grid are circular with a nominal diameter of $30 \mu\text{m}$. This value came out from a compromise between two competing effects that limit the image resolution to $20 \mu\text{m}$: the diffraction effects and the shadowing effect due to the finite size of the pinhole[2].

The digitalized camera image is fitted by a bi-gaussian function of the form

$$I(x, z) = B + A \exp -\frac{1}{2} \left\{ \frac{x'^2}{\sigma_h^2} + \frac{z'^2}{\sigma_v^2} \right\}, \quad (1)$$

where the fitting parameters B_0 , B_x and B_z in the background term $B = B_0 + B_x x + B_z z$ account for spurious background light intensity, A is the intensity amplitude,

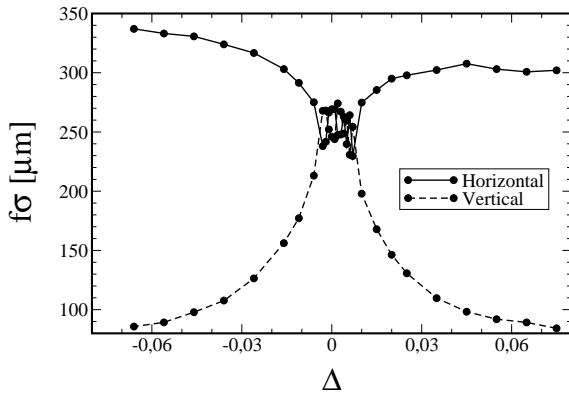


Figure 2: e-beam sizes extracted from fitting of the pinhole image. Solid line corresponds to horizontal beam size and dashed line to the vertical size.

and σ_h and σ_v are the e-beam sizes in the axes rotated by the coupling angle θ :

$$\begin{aligned} x' &= (x - x_0) \cos \theta + (z - z_0) \sin \theta \\ z' &= (z - z_0) \cos \theta - (x - x_0) \sin \theta. \end{aligned}$$

The centroid $\{x_0, z_0\}$ is also a fitting parameter. In Fig.2 we plot σ_h and σ_v as tunes are varied. The wiggler gap is closed in this configuration. Far away from the difference resonance, $\Delta = 0$, the coupling angle is small and the notation σ_h and σ_v is justified: they are respectively the horizontal and vertical beam sizes. In this situation the vertical size is very small because the residual vertical emittance should be negligible. As the resonance is approached, the coupling angle increases and the “horizontal” size diminishes, whereas the “vertical” one increases. This is predicted by the theory of linear coupling[1]. However, very close to the resonance, the two curves display oscillations that are correlated, indicating that there may be some non-trivial emittance exchange in this regime. This behavior may be linked to what some authors have discussed previously[3, 4].

Theory for 2D Source

In this section we will derive the pinhole image that will be formed at the CCD of the $\text{\textcircled{C}}\text{SESO}$ camera. We will compute the image for a 1D source, but the image for the 2D case, in our approximation, can be calculated as the combination of two separate 1D sources. The radiation intensity at point x_2 , located at a distance l_2 away from the source, is given by the integral

$$I(x_2) = \int dx dx' dr' n(x, x') P(r' - x') \delta_p(x(l_1)) \delta_c(x(l_2)), \quad (2)$$

where $n(x, x')$ is the particle distribution function at equilibrium,

$$n(x, x') = \frac{n_0}{2\pi\epsilon_x} \exp\left(-\frac{1}{2}\mathcal{H}\right) \quad (3)$$

$\mathcal{H}(x, x') = (\gamma_x x^2 + 2\alpha_x x x' + \beta_x x'^2)/\epsilon_x$ is the Courant-Snyder invariant function, ϵ_x the equilibrium emittance, δ_p is a delta of Dirac, constraining the geometrical ray to pass through the pinhole at origin, that is, $x(l_1) \equiv x + r'l_1 = 0$. Finally, the function δ_c , also a delta of Dirac, collects all radiation incident on the point x_2 of interest, since it forces $x(l_2) \equiv x + r'l_2 - x_2 = 0$.

The function $P(\theta)$ gives the angular distribution of the radiation intensity. This distribution depends on the e-beam energy and on the energy range to which the camera is sensitive. The distribution function, however, is very much collimated in the forward direction of the e-beam movement and can be very well approximated by a gaussian. There are also filters between the source and the camera that attenuates photons with different energies differently. To estimate the variance σ_γ of this gaussian we can take, as an approximation, the frequency-integrated radiation power. In this case, the variance depends on what plane we consider. The radiation on the plane of the orbit has $\sigma_{\gamma,x} = 0.2705/\gamma$ and the radiation on the perpendicular direction has $\sigma_{\gamma,z} = 0.4473/\gamma$, where γ is the relativistic factor. For the LNLS storage ring, $\gamma \approx 2681$.

The result of the integration in Eq.(2) is a gaussian function in x_2 . Its variance is given by

$$\sigma^2 = \frac{\sigma_x^2}{f^2} \left(\frac{1 + C_1}{(\beta_x \gamma_x - \alpha_x^2) + C_2} \right), \quad (4)$$

which is the same as the source's size $\sigma_x^2 \equiv \epsilon_x \beta_x$, apart from the geometric factor $f \equiv l_1/(l_2 - l_1)$, and correction terms

$$\begin{aligned} C_1 &\equiv (\sigma_{x'}/\sigma_\gamma)^2 / (\beta_x \gamma_x) \\ C_2 &\equiv \left(\frac{\sigma_x/l_1}{\sigma_\gamma} \right)^2 \left\{ 1 - 2(f\tilde{l})\alpha_x + (f\tilde{l})^2 \beta_x \gamma_x \right\}. \end{aligned}$$

that vanish in the limit of small source size. In the expressions above, $\tilde{l} \equiv (l_2 - l_1)/\beta_x$ and $\sigma_{x'} \equiv \gamma_x \epsilon_x$. Given a measured σ^2 , the equilibrium emittance ϵ_x can be calculated from Eq.(4), once the Twiss parameters $\{\alpha_x, \beta_x, \gamma_x\}$ and the beam-line optics $\{l_1, l_2\}$ are known. In Table 1 we list all parameters of the e-beam and of the DXF beam-line that are relevant for calculating emittances from the fitted beam sizes. In order to obtain the coupling strength κ from

Table 1: Nominal Beam and Line Optics at the DXF

Parameter	Value	Parameter	Value
β_x [m]	0.917	β_z [m]	15.27
α_x	-0.22	α_z	-3.68
η_x [m]	0.09	η_z [m]	≈ 0
η'_x	0.26	η'_z	≈ 0
$\sigma_{\gamma,x}$	$0.2705/\gamma$	$\sigma_{\gamma,z}$	$0.4473/\gamma$
E [GeV]	1.37	σ_ϵ [%]	0.076
l_1 [m]	8.5	l_2 [m]	12.75

e-beam size measurements we first note that, within a simple theory of linear coupling in which the tunes are supposed to lie close to a difference resonance, $\nu_x - \nu_z \approx 0$,

the ratio between the vertical and horizontal emittances is related to the coupling strength κ through the following expression[1]:

$$\frac{\epsilon_z}{\epsilon_x} = \frac{\kappa^2}{\kappa^2 + \Delta^2}, \quad (5)$$

where $\Delta \equiv \nu_{0,x} - \nu_{0,z}$ is the uncoupled tunes separation. But the square of the denominator is just the measured tune separation $\delta\nu$, so that the equation can be cast into a more convenient form, $\sqrt{\epsilon_z/\epsilon_x} = |\kappa| \delta\nu^{-1}$, from which $|\kappa|$ can be extracted from a linear fit. The result of this fit is in

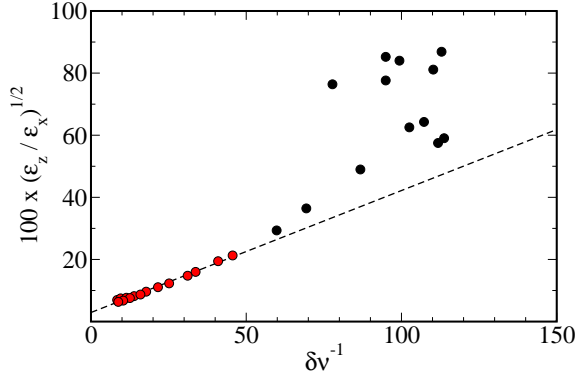


Figure 3: Fitting of coupling parameter from pinhole image. Notice that close to the resonance the measurement of the beam size from the pinhole image leads to emittance oscillations. These points were not considered when fitting a straight line, only the red points were.

Fig. 3. First thing to notice from the plot is that, away from resonance (smaller values of $\delta\nu^{-1}$), the points lie on a straight line and hence the fit is good if it is restricted to this plot region. For points close to the resonance, the simple theory described above can not account for the experimental data. Moreover, despite the fact that away from the resonance the points seem to lie on a straight line, the coupling strength given by fitting, which is $\kappa = 0.39\%$, is considerably smaller than $\kappa = 0.88\%$ obtained from the tune separation. A number of possible pitfalls of the analysis we made so far may be raised: first, we did not consider the pinhole resolution of $20 \mu\text{m}$ from the measurements of σ . If this is done, the discrepancy between one measurement of κ and the other does not improve much. Secondly, the emittances are calculated from the beam sizes assuming that the Twiss parameters are known. In reality there is always some uncertainty around the values in Table 1. But in order to explain the experiments we should have to increase the ratio β_x/β_z , for example, three-fold. This explanation does not seem correct. Thirdly, we did not consider a residual vertical emittance due to a residual vertical dispersion function. This effect would change Eq. (5) in a way that the points in Fig. 3 should not lie on a straight line. This is not the case, obviously.

A plausible explanation for incorrect predictions of our simple theory is the fact that dispersion functions have not been taken into account. They certainly influence the observed e-beam image size. In the next subsection we ana-

lyze how importance this influence is.

Theory for 3D Source

In order to consider the effects of dispersion functions on the image size, we had to extend the integral in Eq. (2) to include the beam 6D phase space. In this case, the action \mathcal{H} appearing in Eq. (3) generalizes to

$$\mathcal{H} = \mathcal{H}_x(x + \eta_x \varepsilon, x' + \eta'_x \varepsilon_x) + \mathcal{H}_z(z, z') + \mathcal{H}_\varepsilon(\varepsilon, \tau), \quad (6)$$

where \mathcal{H}_x and \mathcal{H}_z are the two transverse invariant functions (normalized by the corresponding equilibrium emittances) and $\mathcal{H}_\varepsilon = \varepsilon^2/\sigma_\varepsilon^2 + \tau^2/\sigma_\tau^2$. The integration over τ in the generalization of Eq. (2) can be easily done and only renormalizes the intensity of the pinhole image. The integration over ε , on the other hand, introduces an effective action $\tilde{\mathcal{H}}_x$ for the horizontal phase space[5]:

$$\tilde{\mathcal{H}}_x = (\tilde{\gamma}x^2 + 2\tilde{\alpha}xx' + \tilde{\beta}x'^2)/\varepsilon_x, \quad (7)$$

with

$$\begin{aligned} \tilde{\gamma} &= \gamma_x - (\gamma_x \eta_x + \alpha_x \eta'_x)^2 / \mathcal{G} \\ \tilde{\alpha} &= \alpha_x - (\gamma_x \eta_x + \alpha_x \eta'_x)(\beta_x \eta'_x + \alpha_x \eta_x) / \mathcal{G} \\ \tilde{\beta} &= \beta_x - (\beta_x \eta'_x + \alpha_x \eta_x)^2 / \mathcal{G} \end{aligned}$$

and $\mathcal{G} \equiv \varepsilon_x(\mathcal{H}_x(\eta_x, \eta'_x) + 1/\sigma_\varepsilon^2)$. For 3D sources the same equations in the previous subsection apply. Only now Twiss parameters should be substituted by $\{\tilde{\alpha}, \tilde{\beta}, \tilde{\gamma}\}$. Note that in the 3D case $\tilde{\beta}\tilde{\gamma} - \tilde{\alpha}^2$ in Eq. (4) is not unity. The results from the application of these generalized expressions to the images of the camera are surprisingly very similar to the 2D case (Fig. 3) and do not explain the incorrect value for $|\kappa|$.

CONCLUSIONS

At this point we do not understand the difference between the coupling strength measured from the difference of tunes and the one extracted from pinhole images. In our opinion the most probable cause of this discrepancy is the fact that we performed the integrals over the transverse phase space separately for each direction. This is not rigorously correct since the integrand imposes ties between the two directions. Also, as the resonance is approached, the coupling angle increases. The values of $\sigma_{\gamma,x}$ and $\sigma_{\gamma,z}$ should be corrected accordingly. On the other side, pinhole images reveal a non-trivial emittance exchange very close to the difference resonance. This effect also requires more analysis in order to be properly understood.

REFERENCES

- [1] H. Wiedemann, "Particle Accelerator Physics II", Springer-Verlag Berlin 1999.
- [2] L. Lin, P. Tavares, LNL Report (unpublished).
- [3] K. Ohmi *et al.*, Physical Review E **68**, 751 (1994).
- [4] B. Nash *et al.*, Physical Review ST AB **9**, 032801 (2006).
- [5] X.R. Resende, LNL Report (unpublished).